Investigation of the Impact of Aerosols on Clouds During the May 2003 Intensive Operational Period at the Southern Great Plains

H. Guo, J.E. Penner, and M. Herzog
Department of Atmospheric, Oceanic and Space Sciences
University of Michigan
Ann Arbor, Michigan

Introduction

The effect of aerosols on the clouds, or the so-called aerosol indirect effect (AIE), is highly uncertain (Penner et al. 2001). The estimation of the AIE can vary from 0.0 to -4.8 W/m^2 in global climate models (GCM). Therefore, it is very important to investigate these interactions and cloud-related physical processes further.

The Aerosol Intensive Operational Period (AIOP) at the Southern Great Plains (SGP) site in May 2003 dedicated some effort towards the measurement of the Cloud Condensation Nucleus concentration (CCN) as a function of super-saturation and in relating CCN concentration to aerosol composition and size distribution. Furthermore, airborne measurement for the cloud droplet concentration was also available. Therefore this AIOP provides a good opportunity to examine the AIE. In this study, we use a cloud resolving model (CRM), i.e., Active Tracer High-resolution Atmospheric Model (ATHAM), to discuss the effect of aerosol loadings on cloud droplet effective radius (R_e) and concentration. The case we examine is a stratiform cloud that occurred on May 17, 2003.

The association between the aerosol and the cloud droplet size and number concentration, that is, the AIE, is determined first by the aerosol activation process. The detailed or explicit description of the aerosol activation process in a GCM or a CRM is computationally expensive. Therefore, parameterizing the physical processes, which uses some simple relationships or fundamental physical theories so as to reduce the computational complexity, is often adopted in GCMs and CRMs.

There are various empirical and mechanistic aerosol activation parameterization schemes. The mechanistic schemes are based on physical principals that relate aerosol chemical properties and size distribution, and updraft velocities to the initial cloud droplet number concentration (CDNC). Hence, they are supposed to be more reliable and self-consistent. In this study, three mechanistic nucleation schemes are adopted, i.e., those from Abdul-Razzak and Ghan (2002; AG), Nenes and Seinfeld (2003; NS), and Chuang and Penner (1995; CP) to study the sensitivity of CDNC to the different parameterization schemes.

Model Description and Simulation Setup

The Active Tracer High-resolution Atmospheric Model (ATHAM) (Oberhuber et al. 1998; Herzog et al. 1998; Guo et al. 2004, 2005) is a non-hydrostatic, compressible, formulated with an implicit-time step and finite-difference scheme. A Kessler-type bulk microphysical package is used, except that *Beheng*'s scheme is adopted for the auto-conversion and accretion processes (Herzog 1998; Kessler 1969; Beheng 1994). The AG nucleation scheme (2002) is used in our base case. The model uses a delta-Eddington approximation for the shortwave radiation heating. The longwave radiation code includes parameterizations for absorption by H_2O, O_3, CO_2, and for most of the minor trace gases (N_2O, CH_4, CFCs), as well as the radiative effects of warm clouds (Chou et al. 2001). The surface sensible and latent heat fluxes are from the energy balance Bowen ratio (EBBR) station measurement at the SGP site's Central Facility (CF).

Observations of the cloud micro- and macrophysical properties and radiative properties, as well as the aerosol loading and chemical composition were available from the AIOP. During the time, we examine, the cloud cover was relatively homogeneous following a period of light drizzle that ended at 17:00 Universal Time Coordinates (UTC). Remote sensing retrievals are more credible for relatively homogeneous clouds (Han et al. 1995). So, we mainly compare the simulation results with the measurements after 17:00 UTC to assess the performance of the two-dimensional ATHAM.

The horizontal domain of the model is 210 km and the vertical domain extends from the surface up to 20 km. In the horizontal direction, the grid spacing is uniform, i.e., 2 km; while in the vertical, it is 40 m at the lowest 2 km and then is stretched to about 300 m at the top of the domain (20 km). The initial temperature and water vapor vertical profiles are from the radiosonde sounding at the CF and the initial cloud water content was set to be zero (Figure 1). In this study, the simulation begins at 11:30 a.m. when the radiosonde sounding is available.

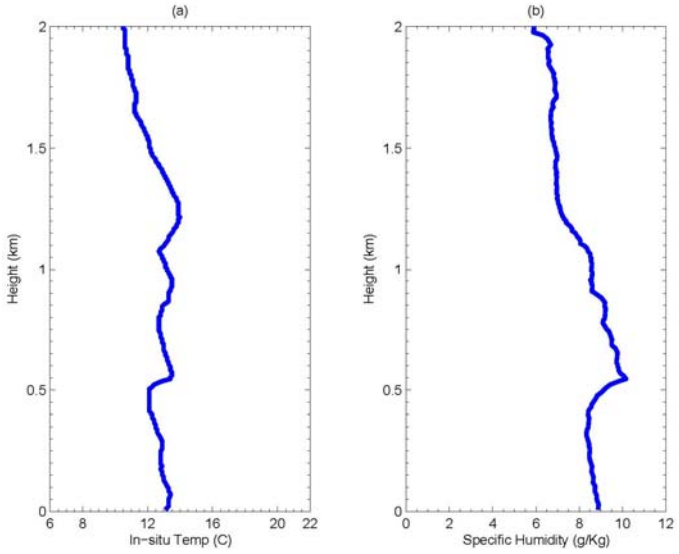

Figure 1. The initial in situ temperature and the moisture vertical profiles from the radiosonde sounding at 11:30 UTC on May 17, 2003.

The large-scale advection for the temperature and moisture are derived from the National Oceanic and Atmospheric Administration Rapid Update Cycle (RUC) data analyses "cropped" over the CF area (Figure 2). For the surface sensible and latent heat fluxes, the EBBR station measurement at the CF is used (Figure 3). The aerosol size distribution was measured by an airborne passive cavity aerosol spectrometer (PCASP). There is also the observed aerosol chemical composition and loading at the CF ground site. The aerosol mixing ratio is assumed to be constant with altitude since the water vapor mixing ratio near the cloud base was within 10% of the ground level value by the ARM radiosonde sounding and airborne measurement (Delene and Deshler 2001; Penner et al. 2004) (Figures 1 and 4). Therefore, the aerosol composition and amount at cloud base are expected to be similar to those measured near the ground.

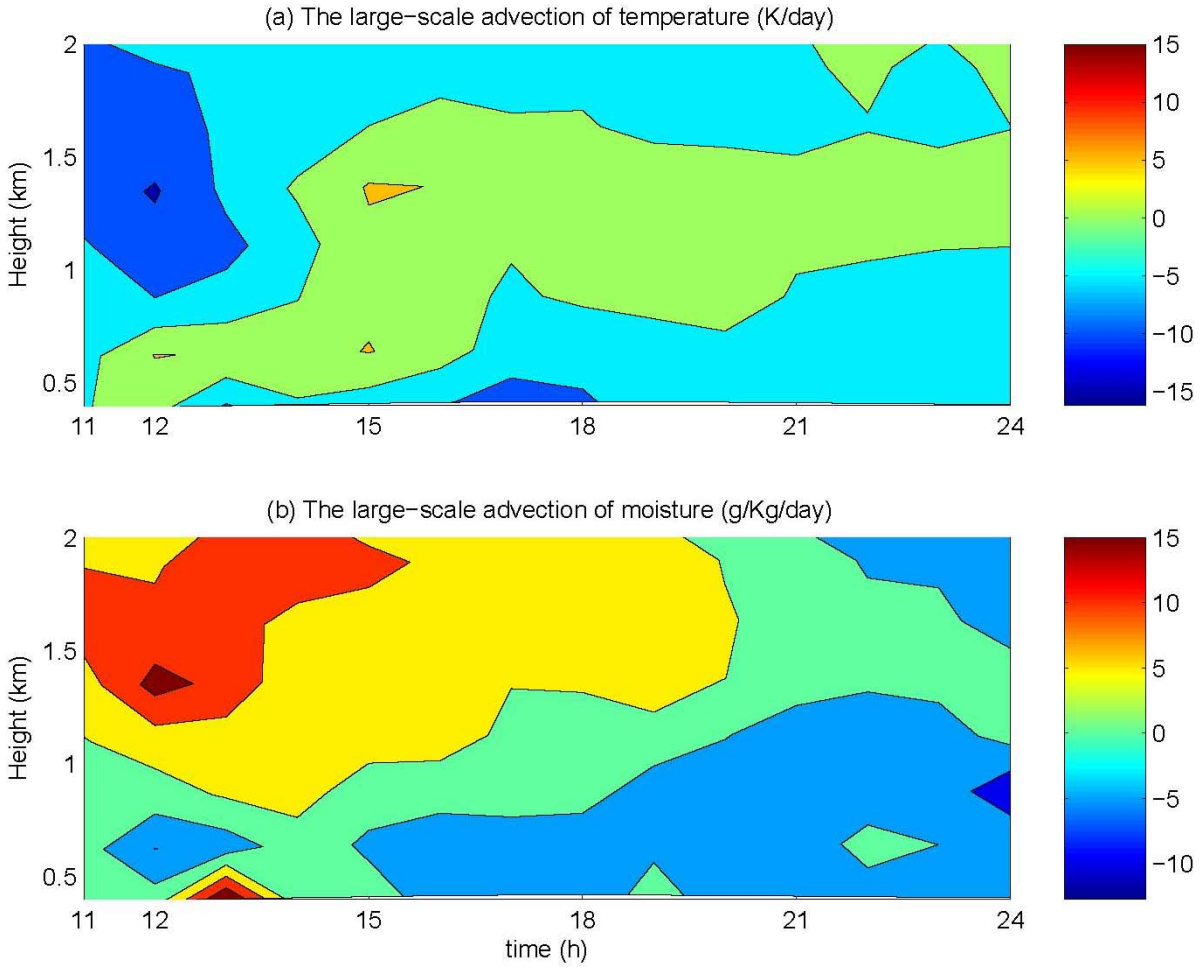

Figure 2. The large-scale advection for the in situ temperature and the moisture derived from the RUC data archive "cropped" over the CF area on May 17, 2003.

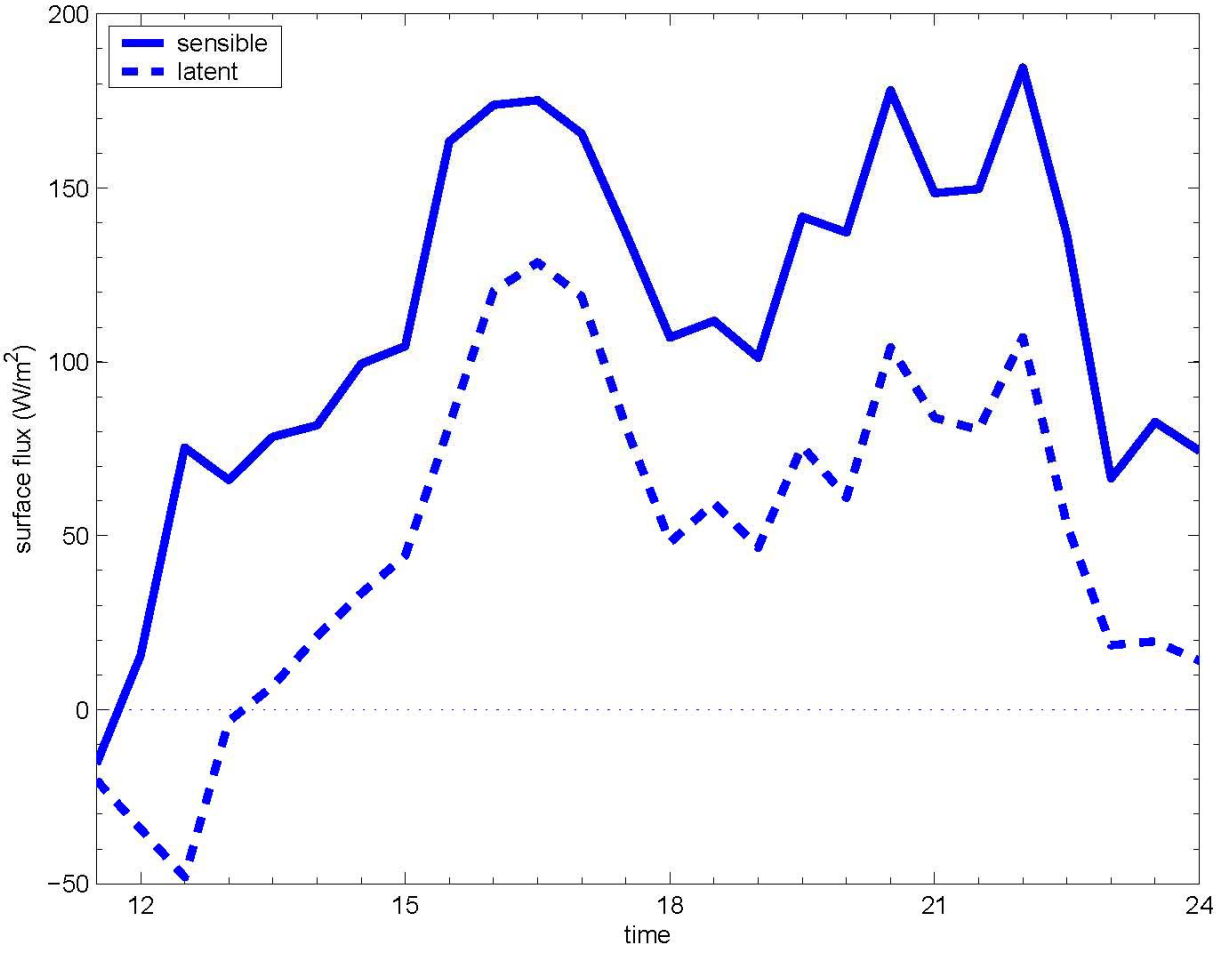

Figure 3. The surface sensible (blue solid) and latent (blue dashed) heat fluxes from the EBBR station measurement at the CF on May 17, 2003.

Numerical Results and Sensitivity Tests

Comparisons with Measurements

Airborne measurements are available near 19:00 UTC, May 17, 2003. To evaluate the credibility of the model results, we first compare the numerical results with the observations. Figure 4a and b depict the vertical profiles of the in situ temperature (T) and the specific humidity (Q) from the airborne measurement and from the ATHAM simulation, respectively. As shown there, ATHAM is able to capture the inversion layer very well. Below the inversion layer, the predicted temperature profile is very close to the measurement. The maximum difference is 0.412°C, which is within one standard deviation of the horizontal variation of the predicted temperature (about 0.796°C). For the moisture profile, the prediction is well within the measurement range below the inversion layer. However, the model fails to simulate the abrupt decrease of the specific humidity at an altitude of 1.75 km. One reason might be the relatively strong moist large-scale advection at this height (Figure 2). Compared to the re-analysis data, the simulated T and Q are much closer to the air borne measurements.

The simulated in situ temperature (T) and the specific humidity (Q) profiles agree favorably with the measurements, which is critical for the simulation of the cloud morphology and the cloud water content. Figure 5 compares the airborne measurement of the CDNC profile with the simulation around 19:00 UTC. We can see that the altitude of the cloud base and cloud top are captured well by ATHAM, mainly due to the good agreement of the T and Q profiles with the observations (Figure 4). At cloud base, the CDNC reaches about 1000/cm^3 in the airborne measurement and 900/cm^3 in the ATHAM simulation, respectively. In the upper part of the cloud, the CDNC reaches about 840/cm^3 and 720/cm^3 in the measurement and simulation, respectively. At altitudes from 0.9 km to 1.0 km, the CDNC suddenly decreases to zero in the observations. ATHAM fails to describe this abrupt change although there is a decrease of CDNC from 900/cm^3 to 680/cm^3.

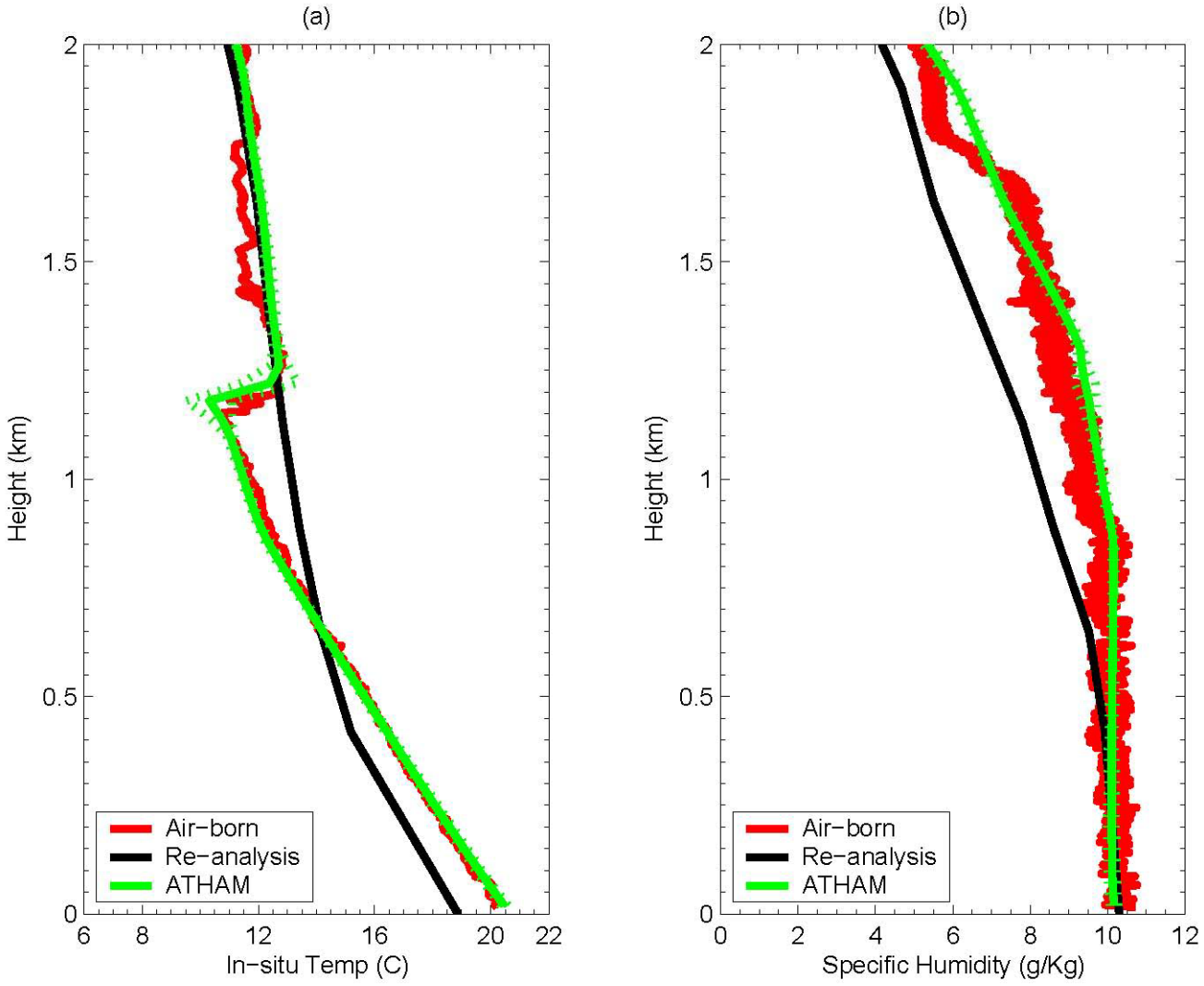

Figure 4. The temperature and the moisture profiles from the air borne measurement (red solid), and the ATHAM simulation (green solid) and its standard deviation (green dotted), and the large-scale re-analysis (black solid) at 19:00 UTC on May 17, 2003.

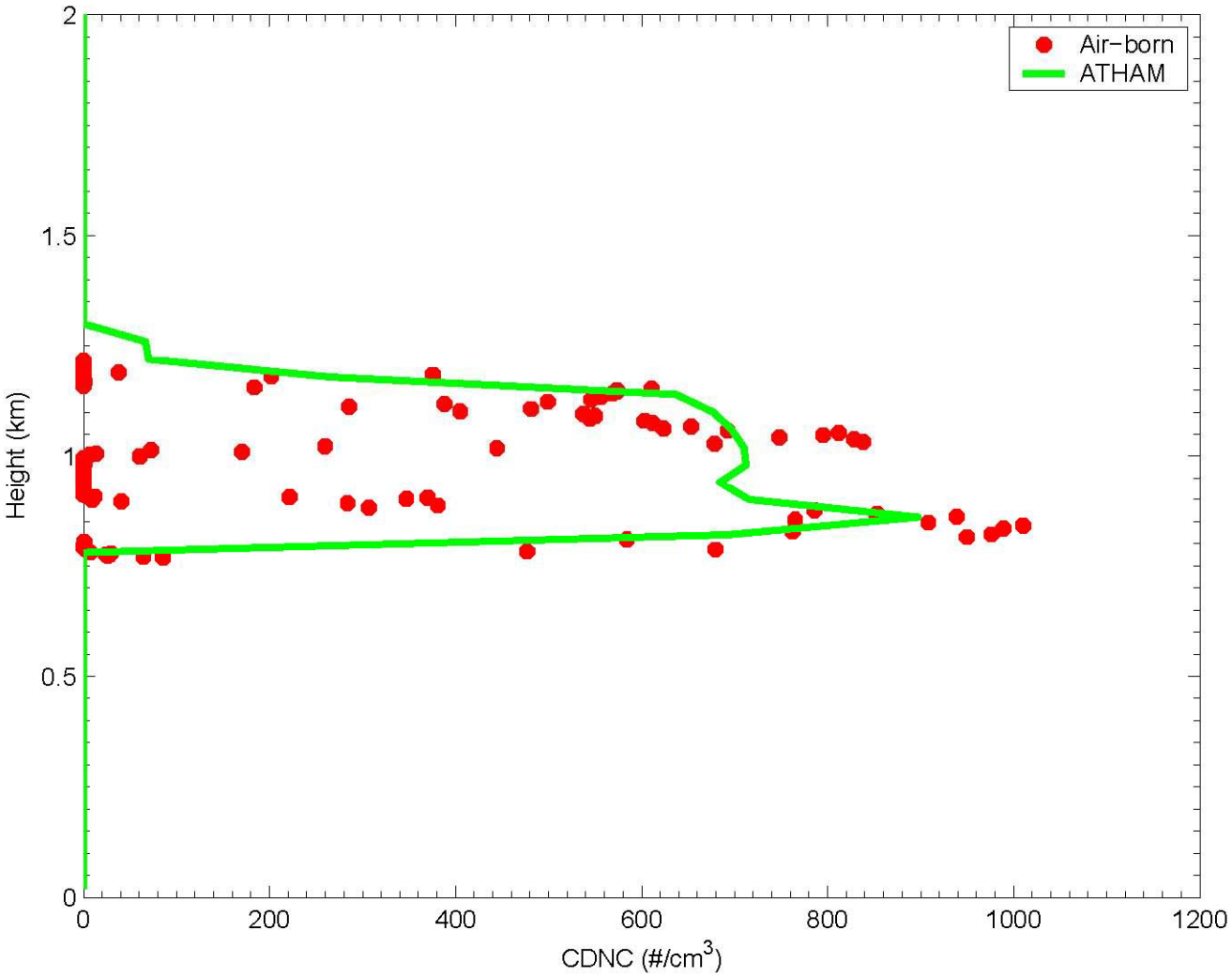

Figure 5. The vertical profile of CDNC from the air borne measurement and the ATHAM simulation around 19:00 UTC on May 17, 2003.

The above comparisons refer to a given time (19:00 UTC). In the following, the temporal evolution of the cloud properties is examined. The cloud morphology is often difficult to simulate in numerical models, especially in single-column models (SCMs) or GCMs (Menon et al. 2003). This is partly due to the coarse resolution and partly due to the deficiencies in cloud parameterizations. However, in this study, ATHAM is able to predict the cloud morphology and its evolution very well. Figure 6b shows the cloud reflectivity from the ground-based millimeter-wavelength cloud radar (MMCR) measurement, which is used to determine the cloud boundaries and retrieve the cloud droplet size. The vertical and temporal variation of the cloud droplet effective radius (R_e) from the ATHAM simulation is showed in Figure 6a.

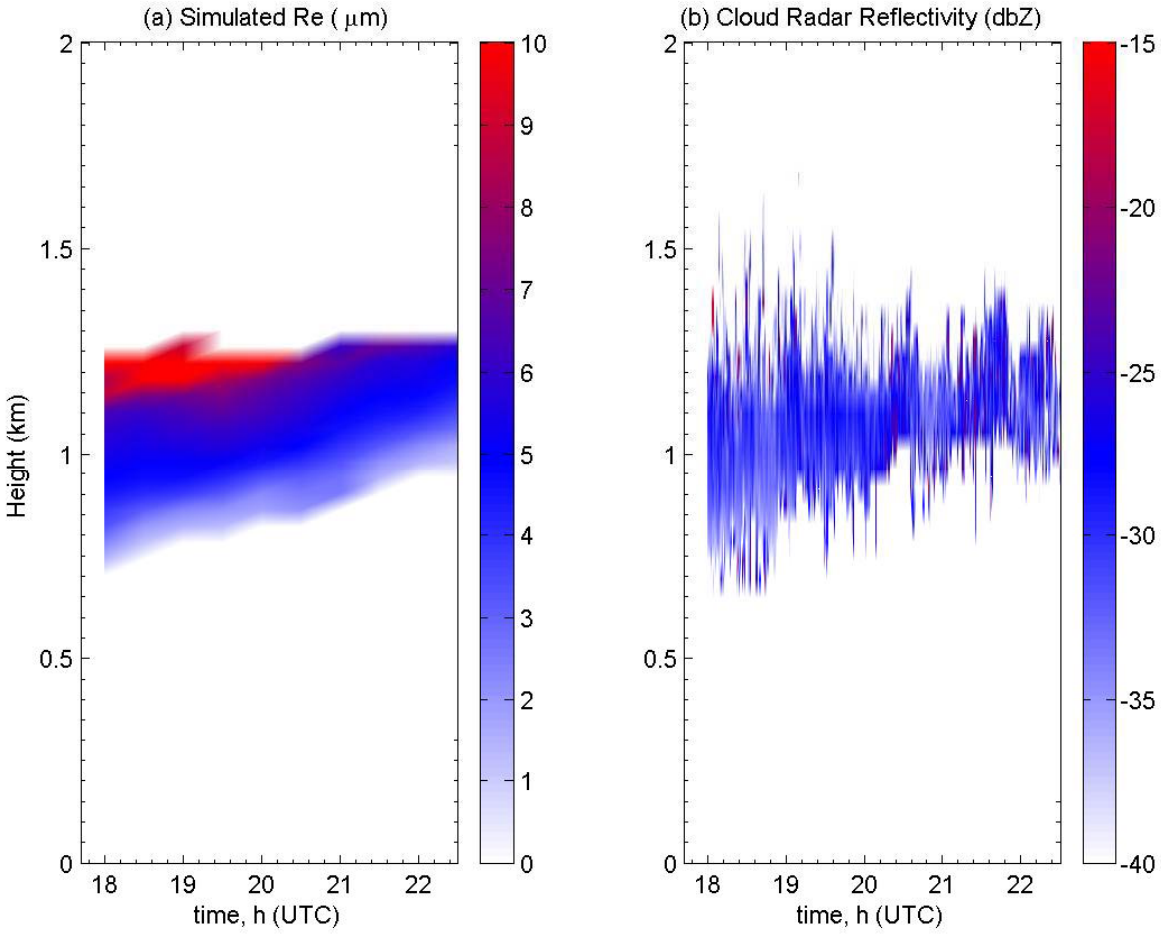

Figure 6. The vertical and temporal variability of the cloud droplet effective radius (R_e) from the ATHAM simulation (a), and the cloud reflectivity from the MMCR measurement (b).

As shown in Figure 6, the predicted cloud top and base, and their evolution is consistent with the measurements. Both cloud top and base rise with time, but cloud base rises faster. From 18:00 UTC to 22:30 UTC, the cloud base increases from 0.70 km to about 0.98 km, but cloud top increases from 1.20 km to about 1.28 km. As a result, the cloud becomes shallower. Moreover, the cloud liquid water content (LWC) tends to decrease, too (Figure 7). Consequently, the cloud liquid water path (LWP) decreases after 20:00 UTC, as well as the cloud optical depth (COD) as a result of the dry large-scale advection and daytime heating (Figure 8). In Figure 7, the best estimate of the cloud base height from the LASER measurement is showed, as well. Again, the simulated cloud base and the observed cloud base are in close agreement. ATHAM can reproduce the general tendency of the cloud morphology evolution although it is not good at capturing the transient fluctuations of cloud top and base. One reason might be that the time interval between simulation results is 0.5 hours. Therefore, some transient fluctuations may not be shown or may be smoothed.

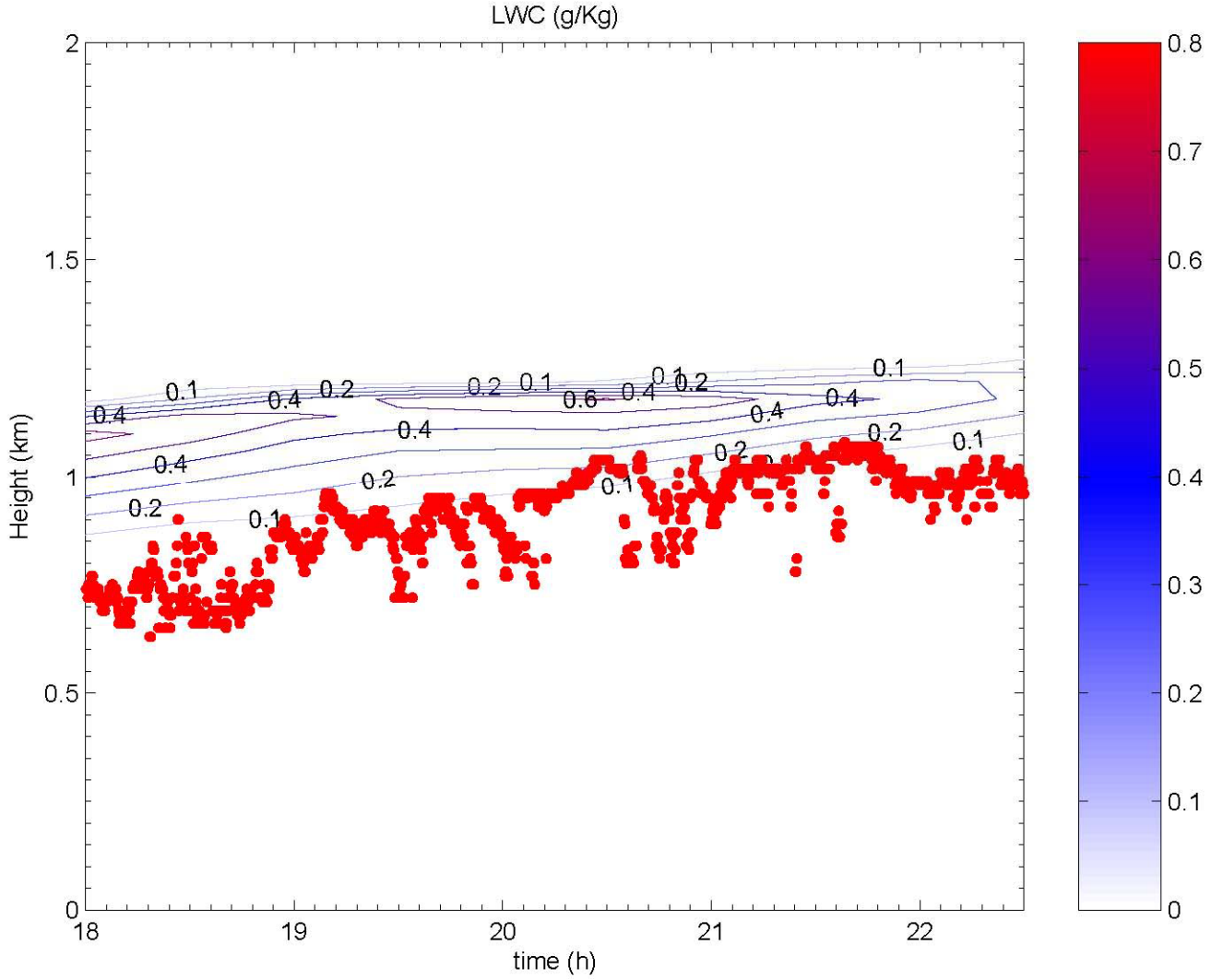

Figure 7. The vertical and temporal variability of the cloud LWC from the ATHAM simulation. The red dots denote the best estimate of the cloud base height from the LASER measurement.

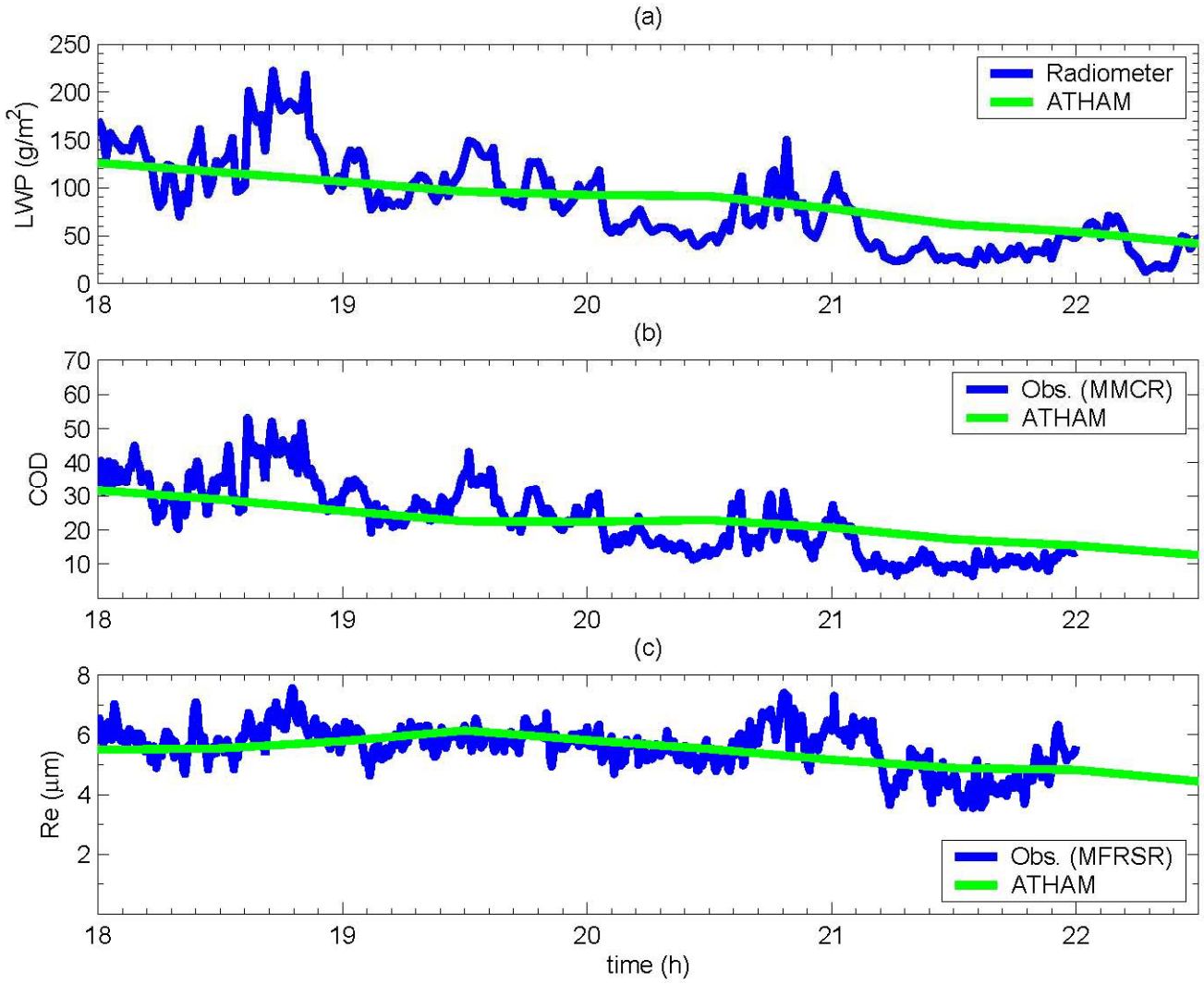

Figure 8. Temporal variability of the cloud LWP, the COD and the cloud droplet R_e from the measurements (blue solid) and the ATHAM simulation (green solid).

During the whole simulation period, the cloud cover remains at nearly 100% from 17:00 UTC to 22:30 UTC, and the cloud properties are relatively horizontally uniform (not shown here).

Sensitivity Tests

The numerical results from the ATHAM simulation compare favorably with the airborne measurements and remote-sensing retrievals. In this section, sensitivity tests are discussed to examine the impact of the different nucleation parameterization schemes on CDNC and the cloud droplet size (R_e), as well as the COD.

Similar to Figure 5, Figure 9 presents the vertical profile of CDNC predicted from three nucleation schemes, the AG scheme, the NS scheme, and the CP scheme. The PCASP only provided the size

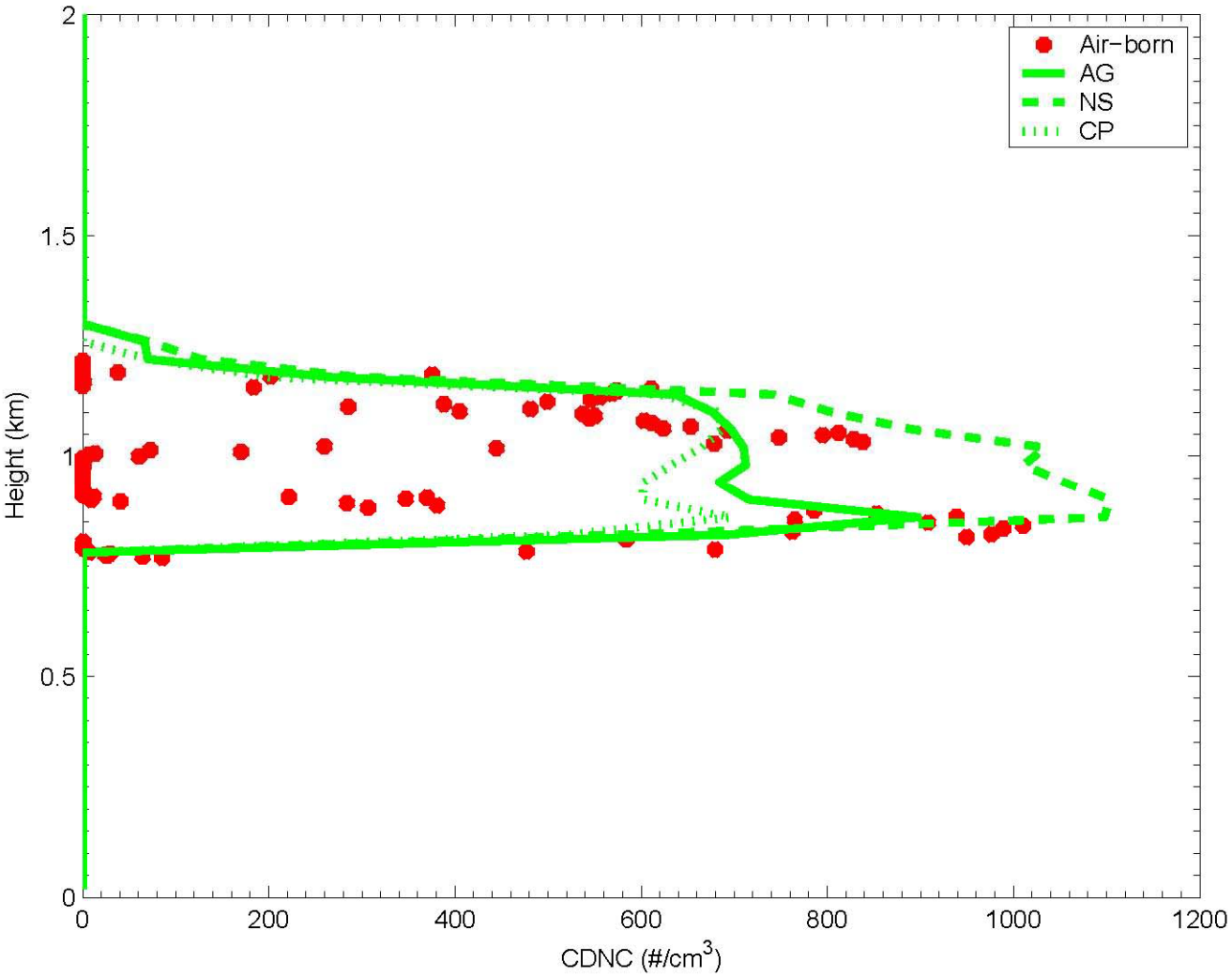

Figure 9. The vertical profile of CNDC from the airborne measurement (red dots), the AG (green solid), the NS (green dashed) and the CP (green dotted) nucleation schemes at 19:00 UTC, May 17, 2003.

distribution of particles whose diameters were greater than 0.1 μm. For the CP scheme, we estimated the total aerosol number concentration which is needed (Chuang and Penner 1995), by using the sulfate amount measured near the ground and assuming that the pre-existing particles followed a superposition of three log-normal distributions.

These three vertical profiles are similar, and are consistent with the airborne measurement. The NS scheme slightly overestimates the CDNC by ~100/cm^3, while the AG scheme and the CP scheme underestimate the CDNC by ~100/cm^3 and 180/cm^3, respectively, especially near cloud base. In these sensitivity tests, the activated aerosol number at the cloud base, from the NS scheme, is the largest, and that from the CP scheme is the smallest.

Figure 10 shows the time evolution of the cloud micro- and macro-physical properties, that is, the CDNC, the cloud LWP, the COD and the cloud droplet R_e from these three tests. All of the test

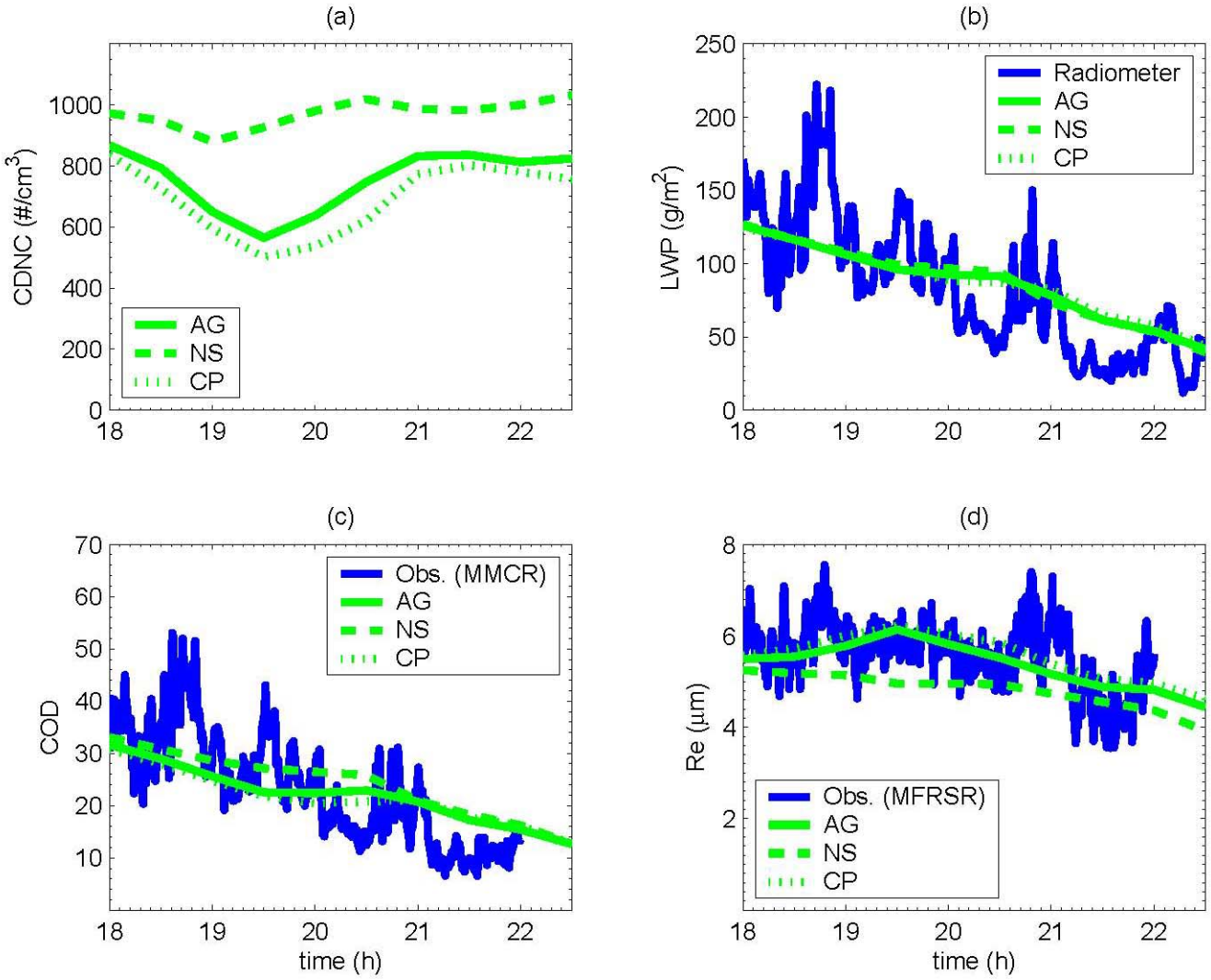

Figure 10. The temporal variability of the cloud CDNC, the cloud LWP, the COD and the Re from the measurements (blue solid), the AG (green solid), the NS (green dashed) and the CP (green dotted) nucleation schemes.

simulations are able to simulate the declining tendency of the LWP and COD because of the dry advection and daytime heating, and the simulated magnitudes are comparable to those observed. From the simulation adopting the NS scheme, the CDNC and COD are larger than the other two simulations, while the R_e is smaller.

However, the cloud LWP remains unchanged using different nucleation schemes, because it is largely determined by the meteorological conditions. Furthermore, there is very little precipitation in all tests due to the small cloud droplet size. Precipitation, therefore, does not help deplete the cloud water.

Conclusion Remarks

The performance of ATHAM in this stratiform cloud case is encouraging. The vertical profile and the time evolution of the cloud morphology, the cloud water content, as well as the cloud droplet size from ATHAM show features that are similar to those observed. The main reason is the agreement between the predicted temperature and moisture profiles from the surface up to the inversion layer with the measurements, which largely determines the thermal and moisture status within clouds.

Different nucleation schemes have little impact on the cloud water content. In this case, the cloud droplet size is so small that there is almost no precipitation to deplete the cloud water. It is mainly determined by the meteorological conditions.

The largest difference of the different nucleation schemes is exhibited through the cloud droplet effective radius and the cloud optical depth. The NS scheme predicts a larger cloud droplet number concentration than the other two schemes. As a result, the cloud droplet size is smaller and the cloud optical depth is larger since the cloud water content remains unchanged.

Contact

Huan Guo, hguo@umich.edu, (734) 764-0564

Acknowledgments

We thank Dr. Shaocheng Xie for providing us with large-scale forcing data and Mr. Yang Chen for providing the Fortran codes for the Nenes-Seinfeld and Abdul-Razaak-Ghan nucleation schemes. This work was supported by the U.S. Department of Energy's Atmospheric Radiation Measurement Program.

References

Abdul-Razzak, H, and S Ghan. 2002. "A parameterization of aerosol activation, 3. Sectional representation." *Journal of Geophysical Research* 107, 4026, doi10.1029/2001JD000483.

Beheng, K. 1994. "A parameterization of warm cloud microphysical conversion processes." *Atmospheric Research* 33, 207-233.

Chou, M, M Suarez, X Liang, and M-H Yan. 2001. A thermal infrared radiation parameterization for atmospheric studies. Tech. rep. *on global modeling and data assimilation*, NASA/TM-2001-104606, Vol.19, Goddard Space Flight Center.

Chuang, C, and J Penner. 1995. "Effect of anthropogenic sulfate on cloud drop nucleation and optical properties." *Tellus* 47, 566-577.

Delene, DJ, and T Deshler. 2001. "Vertical profiles of cloud condensation nuclei above Wyoming." *Journal of Geophysical Research* 106, 12579-12588.

Guo, H, JE Penner, M Herzog, and X Liu. 2004. "Comparison of the vertical velocity used to calculate the cloud droplet number concentration in a cloud resolving and a global climate model." In *The Fourteenth ARM Science Team Meeting Proceeding*, Albuquerque, New Mexico.

Guo, H, JE Penner, and M Herzog. 2005. "Examining the aerosol indirect effect in the second aerosol characterization experiment (ACE-2) with a cloud resolving model." In *the Seventh Conference on the Atmospheric Chemistry, the 85th American Meteorological Society Annual Meeting*, San Diego, California.

Han, Q, W Rossow, R Welch, A White, and J Chou. 1995. "Validation of satellite retrieval of cloud microphysics and liquid water path using observations from FIRE." *Journal of Atmospheric Science* 52(23):4183-4195.

Herzog, M. 1998. Simulation der Dynamik eines Multikomponentensystems am Beispiel vulkanischer Eruptionswolken. Ph.D. thesis, Max-Planck-Institute for Meteorology, Hamburg, Germany.

Herzog, M, H Graf, C Textor, and J Oberhuber. 1998. "The effect of phase changes of water on the development of volcanic plumes." In Report No. 270, Max-Plank Institute for Meteorology.

Kessler, E. 1969. "On the distribution and continuity of water substance in atmospheric circulation." Meteorological Monographs. American Meteorological Society. Vol. 10 No. 32 10, 84.

Menon, S, J-L Brenguier, O Boucher, P Davison, AD Del Genio, J Feichter, S Ghan, S Guibert, X Liu, U Lohmann, H Pawlowska, JE Penner, J Quaas, DL Roberts, L Schuller, and J Snider. 2003. "Evaluating aerosol/cloud/radiation process parameterizations with single-column models and Second Aerosol Characterization Experiment (ACE-2) cloudy column observations." *Journal of Geophysical Research* 108(D24):4762, doi:10.1029/2003JD003902, 003.

Nenes, A, and J Seinfeld. 2003. "Parameterization of cloud droplet formation in global climate models." *Journal of Geophysical Research* 108, 4415, doi:10.1029/2002JD002911.

Oberhuber, J, M Herzog, H Graf, and K Schwanke. 1998. "Volcanic plume simulation on large scales." In Report No. 269, Max-Plank Institute for Meteorology.

Penner JE, M Andreae, H Annegarn, L Barrie, J Feichter, D Hegg, A Jayaraman, R Leaitch, D Murphy, J Nganga, G Pitari, and et al. 2001. "Climatic Change 2001, The Scientific Basis." Chapter 5 Aerosols, their direct and indirect effects, edited by JT Houghton, Y Ding, DJ Griggs, M Noguer, PJ van der Linden, X Dai, K Maskell, and CA Johnson, Report to Intergovernmental Panel on Climate Change from the Scientific Assessment Working Group (WGI). Cambridge University Press, pp. 289-348.

Penner JE, X Dong, and Y Chen. 2004. "Observational evidence of a change in radiative forcing due to the indirect aerosol effect." *Nature* 427(15):231-234.